

# Conversion of carbon dioxide into carbon monoxide using nanosecond pulsed discharges

Naoya Sumi<sup>1</sup>, Takuma Sakamoto<sup>1</sup>, Yuki Akimoto<sup>1</sup>, Takao Namihira<sup>2</sup>, Douyan Wang<sup>2,\*</sup>

<sup>1</sup> Graduate School of Science and Technology, Kumamoto University, Japan

<sup>2</sup> Institute of Industrial Nanomaterials, Kumamoto University, Japan

\* Corresponding author: [douyan@cs.kumamoto-u.ac.jp](mailto:douyan@cs.kumamoto-u.ac.jp) (Douyan Wang)

Received: 23 November 2022

Revised: 13 February 2023

Accepted: 6 March 2023

Published online: 8 March 2023

## Abstract

Consumption of fossil fuels has led to yearly increases in emissions of CO<sub>2</sub>, a main component of the greenhouse gases that contribute to global warming. As such, methods to reduce CO<sub>2</sub> emissions and treat the emitted CO<sub>2</sub> are being researched around the world. One method of interest in treating CO<sub>2</sub> is the use of non-thermal equilibrium plasma, which is low in cost and highly efficient. Nanosecond (NS) pulsed power generators with very short voltage durations of 5 ns have recently been developed. Such power generators feature minimal loss of heat and high electron energy. This study examined the characteristics of NS pulsed discharges when used to convert CO<sub>2</sub> in order to determine its decomposition and conversion efficiency and compare it with other discharge methods. The effects on the CO<sub>2</sub> conversion rate of changing the diameter of the central wire electrode and adding Ar were investigated. It was confirmed that the wire diameter of the central electrode has a significant effect on CO<sub>2</sub> decomposition performance because it changes the nature of the discharge itself. A larger central electrode diameter is suitable for higher CO<sub>2</sub> conversion rates. The addition of Ar had a minimal effect on decomposition performance. A maximum conversion rate of 19.2 % was achieved by NS pulsed discharge, indicating the possibility of contributing to the reduction of CO<sub>2</sub>.

**Keywords:** Carbon dioxide (CO<sub>2</sub>), carbon monoxide (CO), global warming, nanosecond, pulsed discharge.

## 1. Introduction

Environmental problems caused by global warming have become more and more serious in recent years [1], with examples including melting glaciers, extreme weather events, and desertification. The dominant cause of global warming is very likely the increase in greenhouse gases caused by human activities. CO<sub>2</sub> accounts for about 80% of the total greenhouse gas emissions that cause global warming [2]. As such, methods to reduce CO<sub>2</sub> emissions and to treat the emitted CO<sub>2</sub> are being researched around the world. There are two main treatment methods: carbon capture and storage (CCS) and carbon capture and utilization (CCU) [3]. CCS is a technology that captures carbon from industrial processes and stores it in various forms in order to reduce CO<sub>2</sub> emissions from human activities. CCU is a promising technology for sustainable reduction of CO<sub>2</sub> [4]. CO<sub>2</sub> recovered and separated from industrial processes can be converted into value-added materials, including chemical products and fuels.

A technique that is the target of much attention recently is CCU processing of CO<sub>2</sub> using non-thermal equilibrium plasma [4]. Non-thermal equilibrium plasma is a state in which only electron energy is overwhelmingly higher than that of other molecules. In other words, it attempts to realize only the desired reaction via electrons and is a very efficient technology. Non-thermal equilibrium plasmas used for CO<sub>2</sub> conversion include glow discharge [5], corona discharge [6], and DBD discharge [7–9]. Among these, the DBD discharge has attracted considerable attention because of its high CO<sub>2</sub> conversion rate of over 20% and simple structure that can be easily modified for industrial applications. However, it is also considered important to improve energy efficiency from the viewpoint of energy saving. Since nanosecond (NS) pulsed discharges

apply a steep high voltage with a pulse width of 5 ns, the discharge phase does not shift to the glow discharge phase, which would result in minimal loss of heat [10]. Instead, the discharges consist only of streamers that excel in the generation of chemically active species. NS pulsed discharges are proven to be highly energy efficient, surpassing other forms of discharge for ozone generation and other applications [11, 12]

This study examined the effects of changing the nature of NS pulsed discharges on CO<sub>2</sub> conversion and calculated the energy balance of the entire CO<sub>2</sub> conversion process by determining the decomposition efficiency and conversion rate for this method. Specifically, changes in the inner electrode diameter and gas composition were investigated to determine the parameters that are important for improving CO<sub>2</sub> conversion.

## 2. Experimental method

### 2.1 Nanosecond pulsed generator

Fig. 1 shows a schematic diagram of the NS pulsed power generator used in this experiment. The device consists of a spark gap switch (SGS), a triaxial Blumlein line, and a transmission line. For detailed structure and operation, please refer to reference [13]. Fig. 2 shows the voltage and current waveforms during NS pulsed discharge when a coaxial cylindrical reactor is used as a load and filled with 100% CO<sub>2</sub>. Fig. 2 shows that the rise and fall of the voltage is approximately 2 ns and the pulse width is approximately 7 ns, which is close to the theoretical value. The output voltage used in this study was 40 kV, and the range of frequencies used was from 100 pps to 600 pps.

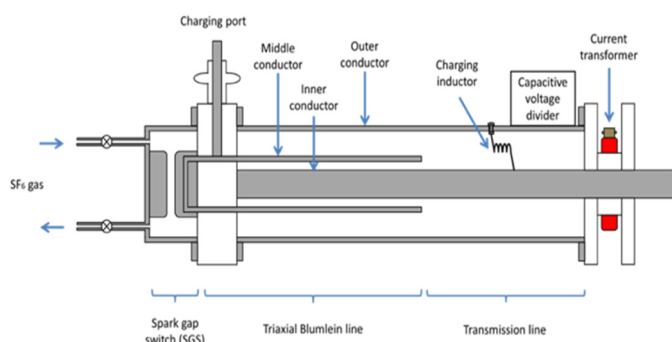


Fig. 1. Schematic diagram of NS pulsed generator.

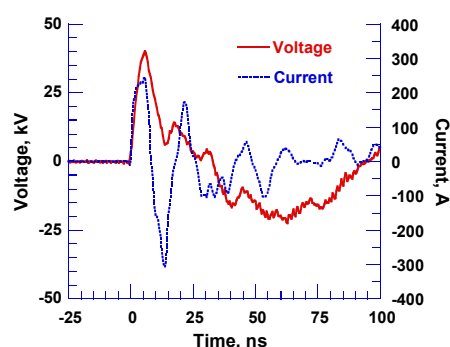
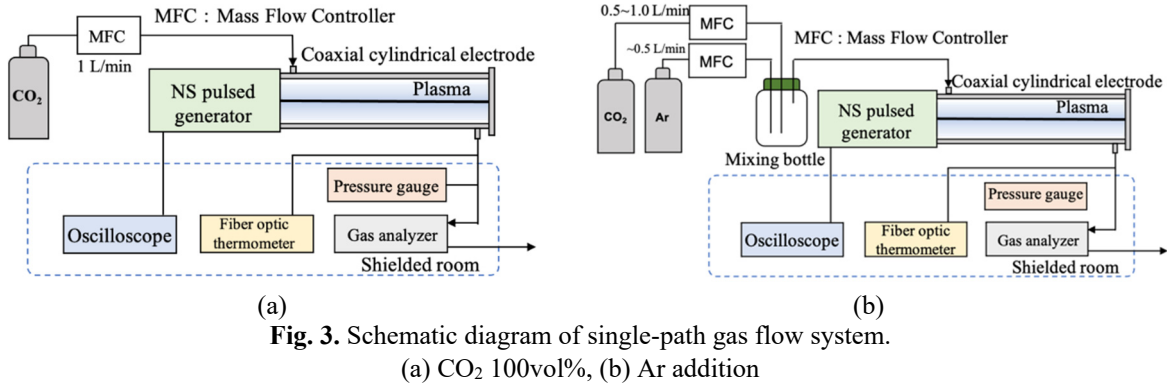


Fig. 2. Voltage and current waveforms of nanosecond pulsed discharge.

### 2.2 Experimental setup

This section describes the experimental system and equipment. Two experimental systems were used in this study: a single-path discharge system in which CO<sub>2</sub> passes through the discharge reactor once, and a circulated discharge treatment in which the gas in the discharge reactor is circulated. Fig.3 (a) and 3 (b) show the schematic diagram used in the single-path discharge treatment. In Fig.3 (a), CO<sub>2</sub> (99.5%) was used as the source gas, and in Fig.3 (b), a mixture of CO<sub>2</sub> plus Ar (99.999%) was used as the source gas. The gas flow rate was controlled at 1.0 L min<sup>-1</sup> using a mass flow controller (SEC(F)-N112MGMW, HORIBA) to flow the gas into the discharge reactor. The reactor shape was a coaxial cylinder. A stainless-steel cylinder with an inner diameter of 76 mm and a length of 1,000 mm was used as the external electrode. A stainless-steel wire was used as the center electrode. The diameter of the center electrode was varied between 0.30, 1.00, 2.00, and 4.00 mm. In Fig.3 (b), the raw material gas flows through a mixing bottle before flowing into the discharge reactor. It passes through the plasma space in the discharge reactor and exits the discharge reactor. The treated sample gas flowed into an infrared gas analyzer (IR202-A, Yokogawa Electric), a device for measuring CO<sub>2</sub>, CO, and O<sub>2</sub> concentrations, before being released from the system. A capacitive voltage divider was mounted on the transmission line between the triaxial Blumlein line and the load to measure the output voltage of the NS pulsed generator in Fig.1. The discharge current through the load was measured using a current transformer (MODEL CT-F1. 0, Bergoz Instrumentation, USA), which was located after the transmission line in Fig.1. Fig. 4 shows the measurement path used for the circulated discharge process. The feed gas was allowed to flow in until the gas analyzer confirms that the path indicated by the red line is filled with CO<sub>2</sub>. The flow rate was

fixed at 1.0 L min<sup>-1</sup>. After that, the inflow of gas from outside was cut off by switching two valves. The pump (BA-110SN, Iwaki) could then be activated to create a system that circulates the gas in the discharge reactor as shown by the blue line. Then, a pulse voltage is applied to the discharge reactor to react with the circulating CO<sub>2</sub>. Center electrode diameters of 0.30, 2.00, and 4.00 mm were used.



**Fig. 3.** Schematic diagram of single-path gas flow system. (a) CO<sub>2</sub> 100vol%, (b) Ar addition

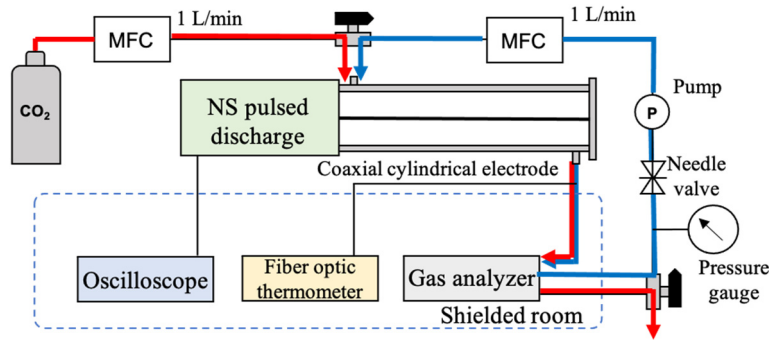


**Fig. 4.** Schematic diagram of circulated gas flow system.

The equations used to evaluate the research results of the next chapter are shown below:

$$IED [J/L] = \frac{E \times f \times 60}{G} \tag{1}$$

$$IED [J/L] = \frac{E \times f \times t}{V} \tag{2}$$

$$DE [g/kWh] = \frac{CO_{2decomposition}}{f \times E \times 10^{-3}} \tag{3}$$

$$X_{CONV} [\%] = \frac{CO_{2input} - CO_{2output}}{CO_{2input}} \times 100 \tag{4}$$

$$X_{eff} [\%] = X_{CONV} \times \frac{CO_{2input}}{CO_{2input} + Ar_{input}} \times 100 \tag{5}$$

Eq. (1) shows the input energy density (IED) in a single-path system. *E* represents energy per pulse [J], *f* represents pulse repetition frequency [pps], and *G* represents gas flow rate [L min<sup>-1</sup>]. Eq. (2) shows the *IED* in a circulating system. *t* is the discharge time [s] and *V* is the total volume of enclosed gas [L]. Eq. (3) shows the CO<sub>2</sub> decomposition efficiency [g kWh<sup>-1</sup>], where *CO<sub>2decomposition</sub>* is the amount of CO<sub>2</sub> decomposed [g h<sup>-1</sup>]. Eq. (4) shows the CO<sub>2</sub> conversion efficiency (*X<sub>CONV</sub>*), where *CO<sub>2input</sub>* is the incoming CO<sub>2</sub> gas [vol%] and *CO<sub>2output</sub>* is the outgoing CO<sub>2</sub> gas [vol%]. Eq. (5) shows the effective conversion efficiency of CO<sub>2</sub> (*X<sub>eff</sub>*). *Ar<sub>input</sub>* is the incoming Ar gas [vol%].

### 3. Results and discussion

#### 3.1 Effect of center electrode wire diameter on CO<sub>2</sub> decomposition in single-path discharge processing

The following are the results of examining the CO<sub>2</sub> decomposition characteristics via NS pulsed discharge using the setup described in Fig. 3 (a). Four center electrode wire diameters were used: 0.30, 1.00, 2.00, and 4.00 mm. Pulse frequency was varied between 100 pps and 600 pps in 100 pps increments. The applied voltage was fixed at 40 kV and the flow rate at 1.0 L min<sup>-1</sup>. Eqs. (6) and (7) represent the decomposition of CO<sub>2</sub> into CO and O when electrons energized by the discharge collide with CO<sub>2</sub> [14]. Eq. (6) has peak collision cross sections around 4 eV and 8 eV, while Eq. (7) has a peak value around 8.5 eV [15, 16].



Fig. 5 shows the dependence of CO<sub>2</sub>, CO, and O<sub>2</sub> concentration changes on center electrode wire diameter. The CO<sub>2</sub> graph indicates a decrease in concentration, while the CO and O<sub>2</sub> graphs indicate increases in concentration. The change in gas concentration increases as the wire diameter of the center electrode increases.

Fig. 6 shows maximum CO<sub>2</sub> decomposition efficiency for each center electrode wire diameter. It shows that the larger the wire diameter, the higher the CO<sub>2</sub> decomposition efficiency. In comparison with reference [17], which modeled CO<sub>2</sub> decomposition by nanosecond pulse discharge at an internal electrode diameter of 1.2 mm, it was found that the CO<sub>2</sub> decomposition efficiency was almost the same at an internal electrode diameter of 1 mm in this experiment. It is also stated from reference [17] that reaction (6) is the reaction that accounts for more than 80% of CO<sub>2</sub> decomposition. Therefore, the experimental results are discussed from the above Eqs. (6) and (7). Fig 6 shows that the larger the wire diameter, the higher the CO<sub>2</sub> decomposition efficiency. Because the electric field in the vicinity of the large-diameter electrode is smaller than that of the narrow-diameter electrode, the time until the streamer head is formed is longer for the large-diameter electrode [18]. As a result, the voltage at the time of streamer head formation is larger [10], so the streamer head has a higher electric field and propagates faster [18–20]. So, the temperature of the electrons produced at the large diameter electrode is also higher, and the reaction in Eqs. (6) and (7) is more active. As a result, the CO<sub>2</sub> decomposition efficiency is higher.

However, arc discharges were observed at 400 pps with a wire diameter of 4.0 mm but were not observed at diameters of 2.0 mm or smaller. While an increase in CO<sub>2</sub> decomposition efficiency is expected as the inner electrode diameter increases, the transition to arc discharge occurs earlier. In this study, it was observed that the current value increased with larger inner electrode diameters, and this is thought to be the reason for the early transition to arc discharge at 4.0 mm.

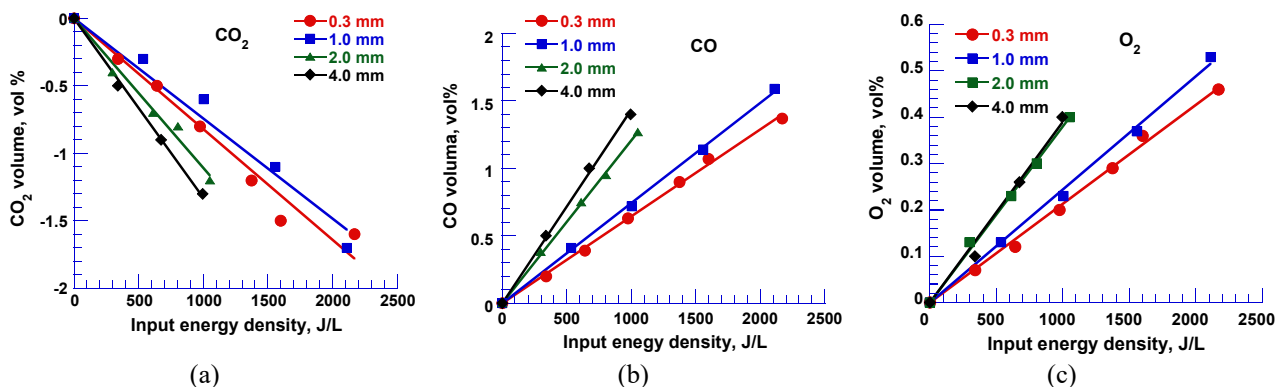


Fig. 5. Dependence of CO<sub>2</sub>, CO, and O<sub>2</sub> concentration changes on the IED at each center electrode wire diameter. (a) CO<sub>2</sub> (b) CO (c) O<sub>2</sub>

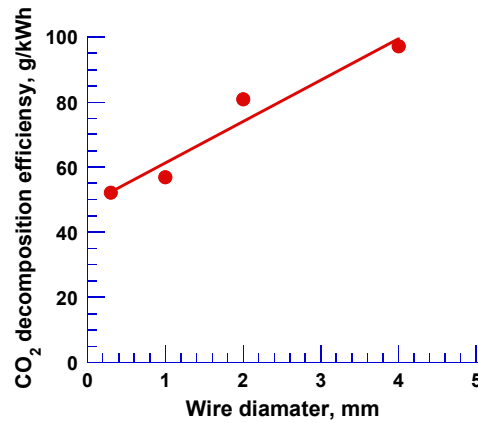


Fig. 6. CO<sub>2</sub> decomposition efficiency at each center electrode wire diameter.

### 3.2 Effect of Ar addition on CO<sub>2</sub> decomposition in single-path discharge processing

This section examines the results of CO<sub>2</sub> decomposition via NS pulsed discharge as shown in Fig. 3 (b) when Ar gas is added. Ar gas has a metastable state above the ionization energy of CO<sub>2</sub>, which is expected to broaden the discharge region and increase the discharge current, etc [21, 22]. In this chapter, we investigated the usefulness of changing the gas composition by using Ar gas for CO<sub>2</sub> decomposition in NS pulsed discharges. The applied voltage was 40 kV, the flow rate was 1.0 L min<sup>-1</sup>, the wire diameter of the center electrode was 4.0 mm, and the frequency was increased from 200 pps to 600 pps in 100 pps increments. The following CO<sub>2</sub> : Ar ratios were used: 10:0, 8:2, 7:3, 6:4, and 5:5. Increasing the ratio of Ar led to a decrease in the initial concentration of CO<sub>2</sub>, resulting in a higher conversion efficiency in Eq. (4). The effective conversion efficiency to the IED at each gas ratio was derived using Eq. (5). Fig. 7 shows the voltage, current, and energy waveforms. As is evident in Fig. 7, there is no difference in the voltage waveform due to the addition of Ar. However, the current and energy values increase slightly with the addition of Ar. It was confirmed in this and previous studies that Ar addition contributed to the increase in current and energy value [21].

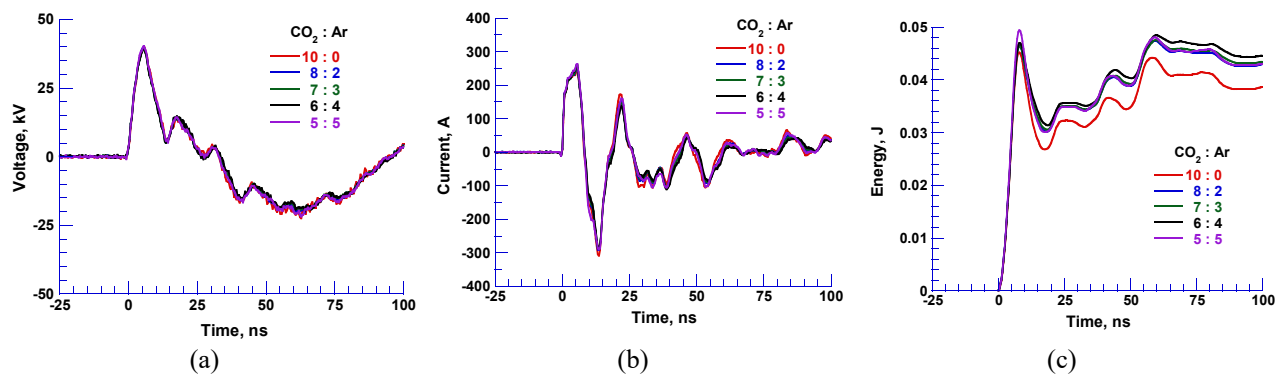


Fig. 7. Voltage and current waveforms when argon is added.

(a) = voltage, (b) = current, (c) = energy

Fig. 8 shows the effective conversion efficiency of CO<sub>2</sub> when Ar is added. The graph shows the effective conversion efficiency of CO<sub>2</sub> when Ar is added. The graph shows that Ar has no effect on the effective conversion efficiency of CO<sub>2</sub>. taking into account the error of the infrared gas analyzer ( $\pm 1$  % FS) and the fact that there is no proportional relationship between the ozone decomposition efficiency and the rate of Ar addition This result is similar to the results of the CO<sub>2</sub> decomposition study reported by Moss *et al.* [21]. The study done by Moss compares experimental results with numerical simulations based on modeling [21]. We used Eq. (8), the reaction rate Eq. (6), to examine the cause [22]. From Fig. 7, the difference in current value due to the addition of Ar is about 10 A, so the  $[e]$  value is considered to be almost the same. In the case of CO<sub>2</sub> : Ar = 5 : 5, the value of reaction rate constant  $k$  is twice that of CO<sub>2</sub> : Ar = 10 : 0, but the  $[CO_2]$  value is 1 / 2 that of CO<sub>2</sub> : Ar = 10 : 0 [22]. These results indicate that  $[CO_2]_{\text{decomposition}}$  is equivalent with and without

the addition of Ar. Therefore, it is concluded that CO<sub>2</sub> decomposition with Ar is not effective.

$$[CO_2]_{decomposition} = k[CO_2][e] \tag{8}$$

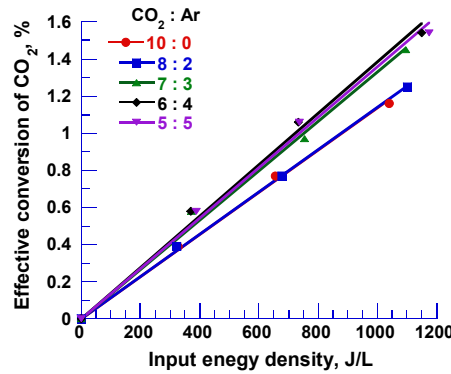


Fig. 8. Effective conversion rate of CO<sub>2</sub> when Ar is added.

### 3.3 Effect of center electrode wire diameter on CO<sub>2</sub> decomposition in circulated discharge processing

The following are the results of CO<sub>2</sub> decomposition via NS pulsed discharge when the wire diameter of the center electrode in Fig. 4 was varied from 0.30, 2.00, and 4.00 mm. CO<sub>2</sub> was used as the source gas and flowed into the discharge reactor through a mass flow controller at a flow rate of 1.0 L min<sup>-1</sup>. The applied voltage was set at 40 kV. Frequency was set at a constant value determined to have a low possibility of transition to arc discharge based on the discharge in the single-path process for each wire diameter. For wire diameters of 0.3 and 2.0 mm, 400 pps was used. For 4.0 mm, 300 pps was used.

Fig. 9 shows the dependence of CO<sub>2</sub>, CO, and O<sub>2</sub> concentrations on the IED at each center electrode diameter when using the circulated gas flow system. It shows that the level of concentration increase/decrease decreased with higher IED, and a trend for saturation in the concentration of each chemical species was observed. I think there are three causes of this phenomenon: The first is decrease in the CO<sub>2</sub> decomposition rate shown in Eqs. (6) and (7) associated with the decrease in the amount of CO<sub>2</sub>. The second is a decrease in electron density due to electron attachment with oxygen. The third is an increase in recombination reaction between O atoms and CO to form CO<sub>2</sub>. For the 0.3 mm and 2.0 mm wires, the maximum conversion efficiency of CO<sub>2</sub> was 14.2% and 18.2% after 120 minutes of discharge treatment. For the 4.0 mm wire, the maximum CO<sub>2</sub> conversion efficiency was 19.2% after 100 minutes of discharge treatment. These results indicate that a larger wire diameter leads to higher efficiency of CO<sub>2</sub> decomposition.

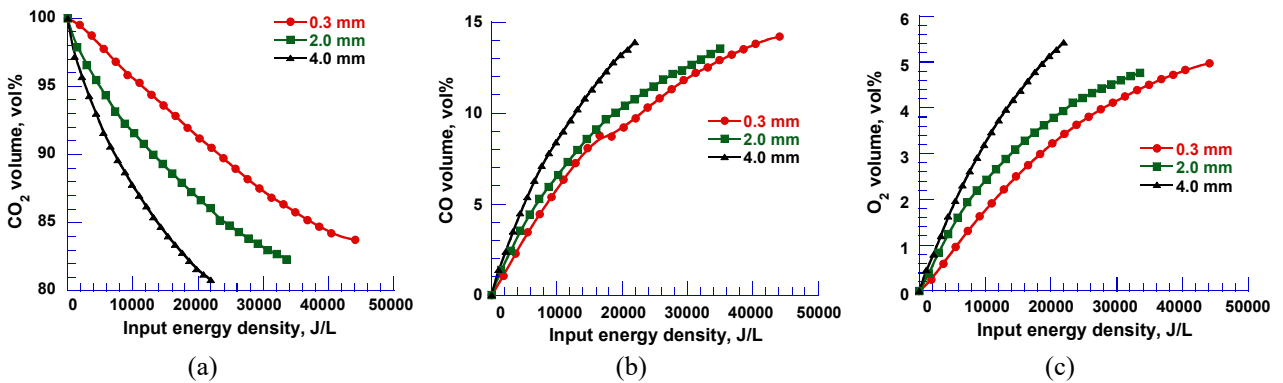


Fig. 9. CO<sub>2</sub>, CO, O<sub>2</sub> concentration for each IED at each center electrode wire diameter.

(a) CO<sub>2</sub> (b) CO (c) O<sub>2</sub>

Fig. 10 shows CO<sub>2</sub> decomposition efficiency with respect to IED. It shows that the CO<sub>2</sub> decomposition

efficiency gradually decreases with time for center electrode diameters of 2.0 mm and 4.0 mm. On the other hand, the CO<sub>2</sub> decomposition efficiency is almost constant when the center electrode diameter is 0.3 mm. From Fig. 9, the slope of CO<sub>2</sub> decomposition decreases as the IED increases, which leads to the decrease in decomposition efficiency in Fig. 10. At a wire diameter of 4.0 mm, the CO<sub>2</sub> decomposition efficiency exceeded 38 g kWh<sup>-1</sup> (red line in Fig.10), which is the CO<sub>2</sub> emission value calculated from all energy consumed in the use of solar power source, from mining of raw materials to maintenance of power generation facilities, etc [23]. This indicator is the maximum CO<sub>2</sub> emission when a renewable energy power source is used and was used as a reference value for the practical application of NS pulsed discharges.

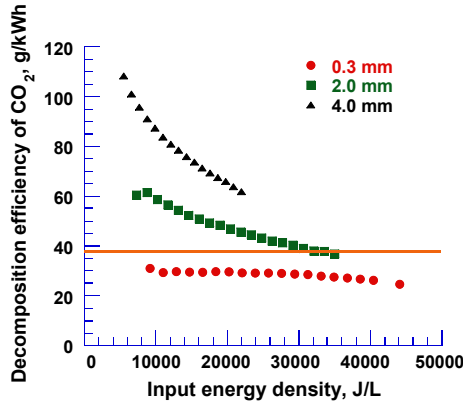


Fig. 10. CO<sub>2</sub> decomposition efficiency with respect to IED.

Fig. 11 shows the dependence of concentration mass balance on IED at each wire diameter. This shows that CO<sub>2</sub> is converted to only CO and O<sub>2</sub> by the discharge. Similar results have been obtained in previous research [24].

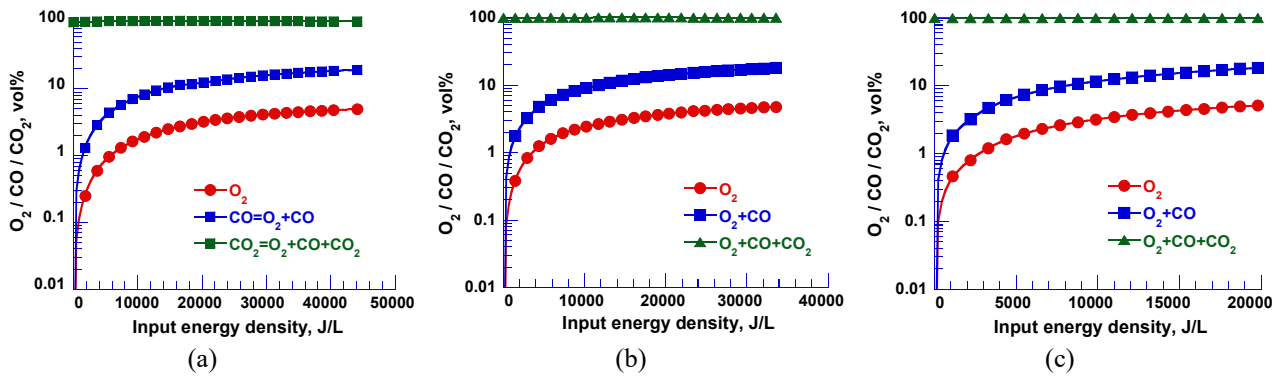


Fig. 11. Dependence of concentration mass balance on IED at wire diameter (a) 0.3 mm, (b) 2.0 mm, (c) 4.0 mm.

### 3.4 Examination of CO<sub>2</sub> recycling processes

Fig. 12 summarizes the results of this paper and results from other studies on CO<sub>2</sub> decomposition using different discharge methods. The chart shows that increasing the wire diameter of the internal electrode in this study succeeded in obtaining a much higher decomposition efficiency than other discharge methods. In addition, the circulated discharge process with the larger wire diameter achieved a higher conversion rate than our previous studies, it is important to note that the experiments in this study were stopped due to the limit of flammability of CO gas being 12.5% [25]. This means that improvements in safety will enable even higher CO<sub>2</sub> conversion rates.

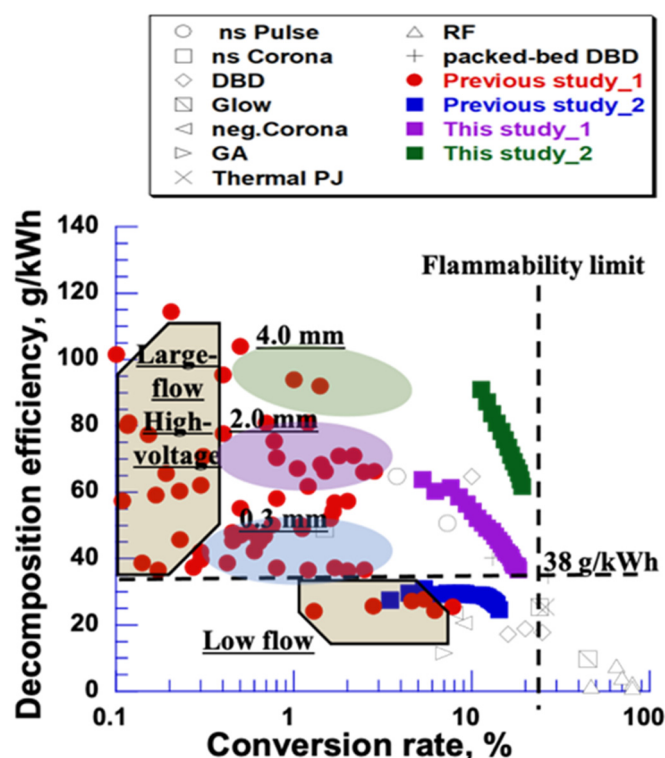


Fig. 12. CO<sub>2</sub> decomposition performance map.

This study has focused mainly on decomposition of 100% CO<sub>2</sub>. However, factory exhaust contains nitrogen, nitrogen oxides, and sulfur oxides, making it necessary to separate and recover CO<sub>2</sub> from mixed exhaust gases. The CO produced by CO<sub>2</sub> decomposition using the method in this study must also be separated and recovered from the resulting gas mixture, which contains both CO<sub>2</sub> and O<sub>2</sub> as well.

Table 1 shows the energy efficiency balance in the conversion of CO<sub>2</sub> into usable resources, including the results obtained in this study. The chemical absorption method, the most common conversion method, is used for CO<sub>2</sub> separation and recovery from power plant exhaust gas [26]. Flue gases containing CO<sub>2</sub> emitted from a power plant or other facility is fed into a separation and recovery plant to recover high purity CO<sub>2</sub> (approximately 99.9%). This chemical absorption method using amines requires 0.14 kWh kg<sup>-1</sup>-CO<sub>2</sub>, as shown in Table 1 [26]. The collected CO<sub>2</sub> is decomposed by the method in this study to produce CO and O<sub>2</sub>. The energy required for CO<sub>2</sub> decomposition is 16.2 kWh kg<sup>-1</sup>-CO<sub>2</sub> (using the circulated discharge treatment with 4.0 mm wire in Fig. 9) and yields about 15% CO. The gas after treatment is separated to recover only CO by adsorption. Recently developed adsorption methods using porous media can recover more than 95% of CO by repeated adsorption and desorption, even at low concentrations of CO. The pressure adsorption method process requires 0.304 kWh kg<sup>-1</sup>-CO<sub>2</sub> as shown in Table 1 [27].

**Table 1.** Energy balance in the conversion of CO<sub>2</sub> into usable resources.

Process stages	Required energy
CO <sub>2</sub> separation and recovery (Chemical absorption method)	0.14 kWh kg <sup>-1</sup> [26] 0.84%
CO <sub>2</sub> decomposition (NS pulsed discharge)	16.2 kWh kg <sup>-1</sup> 97.33%
CO separation and recovery (Pressure adsorption method)	0.304 kWh kg <sup>-1</sup> [27] 1.83%
Total (energy efficiency)	16.6 kWh kg <sup>-1</sup> -CO <sub>2</sub> (60.1 g kWh <sup>-1</sup> )
CO <sub>2</sub> emissions per kWh (Solar power source)	38 g kWh <sup>-1</sup> [23]

By adding the energy efficiencies of the three processes listed in Table 1, the total energy efficiency is calculated to be  $16.6 \text{ kWh kg}^{-1}$ . This means that 1 kWh of electricity can decompose 60.1 g of  $\text{CO}_2$ . Subtracting  $38 \text{ g kWh}^{-1}$ , which is the  $\text{CO}_2$  emission when using solar power, the results indicate that 1 kWh of electricity can contribute to a reduction of approximately 22 g of  $\text{CO}_2$ . This total energy efficiency was used to derive the percentage of energy consumption for each process. The percentage of energy consumption for each process is also shown in Table 1. In the three processes, the  $\text{CO}_2$  decomposition process accounts for more than 97% of the total electricity consumed in the conversion of  $\text{CO}_2$  into usable resources. This stresses the importance of improving the efficiency of  $\text{CO}_2$  decomposition.

#### 4. Conclusion

This study examined the effect of changing experimental parameters when using NS pulsed discharges to convert  $\text{CO}_2$ , derived the decomposition efficiencies and conversion rates of this method, and compared energy efficiencies for each step in the entire process.

In the future, we would like to experiment with thicker wires. In the circulated discharge process, selection of better discharge conditions (e.g., flow rate, voltage) may further improve efficiency.

#### Acknowledgment

This work was partially supported by JSPS KAKENHI Grant Number 19H05611.

#### References

- [1] Specht E., Redemann T., and Lorenz N., Simplified mathematical model for calculating global warming through anthropogenic  $\text{CO}_2$ , *Int. J. Thermal Sci.*, Vol. 126, pp. 1–8, 2016.
- [2] Climate Change 2022., Mitigation of Climate Change. Working Group III contribution to the Sixth Assessment Report of the Intergovernmental Panel on Climate Change, IPCC, 2022.
- [3] Bruhn T., Naims H., and Olfe-Krautlein B., Separating the debate on  $\text{CO}_2$  utilisation from carbon capture and storage, *Environ. Sci. Policy.*, Vol. 60, pp. 38–43, 2016.
- [4] Li S., Ongis M., Manzolini G., and Gallucci F., Non-thermal Plasma-assisted capture and conversion of  $\text{CO}_2$ , *Chemical Eng. J.*, Vol. 410 (15), 128335, 2020.
- [5] Horvath G., Skalny J.D., and Mason N.J., FTIR study of decomposition of carbon dioxide in dc corona discharges, *J. Phys. D: Appl. Phys.*, Vol. 41 (22), 225207, 2008
- [6] Brock S.L., Shimojo T., Marquez M., Marun C., Steven L. Suib S.L., Matsumoto H., and Hayashi Y., Factors influencing the decomposition of  $\text{CO}_2$  in AC fan-type plasma reactors: frequency, waveform, and concentration effects, *J. Catal.*, Vol. 184 (1), pp.123–133, 1999.
- [7] Adrianto D., Sheng Z., and Nozaki T., Mechanistic study on nonthermal plasma conversion of  $\text{CO}_2$ , *Int. J. Plasma Environ. Sci. Technol.*, Vol. 14 (1), e01003, 2020.
- [8] Paulussen S., Verheyde B., Tu X., De Bie C., Martens T., Petrovic D., Bogaerts A., and Sels B., Conversion of carbon dioxide to value-added chemicals in atmospheric pressure dielectric barrier discharges, *Plasma Sources Sci. Technol.*, Vol. 19 (3), 034015, 2010.
- [9] Mei D., and Tu X., Conversion of  $\text{CO}_2$  in a cylindrical dielectric barrier discharge reactor: Effects of plasma processing parameters and reactor design, *J. CO<sub>2</sub> Util.*, Vol. 19, pp. 68–78, 2017.
- [10] Ryu T., Wang D., Namihira T., Behavioral characteristics of nanosecond pulsed discharge in coaxial electrodes, *IEEJ Trans. Fundamentals and Materials (Denki Gakkai Ronbunshi A)*, Vol. 139 (10), pp. 445–452, 2020.
- [11] Wang D., Matsumoto T., Namihira T., and Akiyama H., Development of higher yield ozonizer based on nanoseconds pulsed discharge, *J. Adv. Oxid. Technol.*, Vol. 13 (1), pp. 71–78, 2010.
- [12] Kodama S., Matsumoto S., Wang D., Namihira T., and Akiyama H., Persistent organic pollutants treatment in wastewater using nanosecond pulsed non-thermal plasma, *Int. J. Plasma Environ. Sci. Technol.*, Vol. 11 (2), pp. 138–143, 2018.
- [13] Wang D., Namihira T., and Akiyama H., Recent progress of nano-seconds pulsed discharge and its applications, *J. Adv. Oxid. Technol.*, Vol. 14 (1), pp. 131–137, 2011.
- [14] Aerts R., Somers W., and Bogaerts A., Carbon dioxide splitting in a dielectric barrier discharge plasma: a combined

- experimental and computational study, *ChemSusChem.*, Vol. 8 (4), pp. 702–716, 2015.
- [15] Postler J., Vizcaino V., Denifl S., Zappa F., Ralser S., Daxner M., Illenberger E., and Scheier P., Electron attachment to CO<sub>2</sub> embedded in superfluid he droplets, *J. Phys. Chem. A.*, Vol. 118 (33), pp. 6553–6559, 2014.
- [16] Spencer L. F. and Gallimore D., Efficiency of CO<sub>2</sub> dissociation in a radio-frequency discharge, *Plasma Chem. Plasma Proc.*, Vol. 31, pp. 79–89, 2010.
- [17] Heijkers S., Martini L. M., Dilecce G., Tosi P., and Bogaerts A., Nanosecond pulsed discharge for CO<sub>2</sub> conversion: Kinetic modeling to elucidate the chemistry and improve the performance, *J. Phys. Chem. C.*, Vol. 123 (19), pp. 12104–12116, 2019.
- [18] Nagata Y., Wang D., and Namihira T., Streamer head observation in a wire-plate electrode with varied wire electrode diameters, *Int. J. Plasma Environ. Sci. Technol.*, Vol. 12 (1), pp. 22–29, 2018.
- [19] Komuro A., Takahashi K., and Ando A., Numerical simulation for the production of chemically active species in primary and secondary streamers in atmospheric-pressure dry air, *Journal of Physics D: Applied Physics.*, Vol. 48(22), pp. 215203, 2015.
- [20] Tochikubo F., and Arai H., Numerical simulation of streamer propagation and radical reactions in positive corona discharge in N<sub>2</sub>/NO and N<sub>2</sub>/O<sub>2</sub>/NO, *Jpn. J. Appl. Phys.*, Vol. 41 (2R), pp. 844–852, 2002.
- [21] Moss M S., Yanallah K., Allen R W K., and Pontiga F., An investigation of CO<sub>2</sub> splitting using nanosecond pulsed corona discharge: effect of argon addition on CO<sub>2</sub> conversion and energy efficiency, *Plasma Sources Sci. Technol.*, Vol. 26 (3), 035009, 2017.
- [22] Aerts R., Martens T., and Bogaerts A., Influence of vibrational states on CO<sub>2</sub> splitting by dielectric barrier discharge, *J. Phys. Chem. C.*, Vol. 116 (44), pp. 23257–23273, 2012.
- [23] Imamura E., Iuchi M., and Bando S., Comprehensive assessment of life cycle CO<sub>2</sub> emissions from power generation technologies in Japan, *CRIEPI Ed.*, No. Y06, 2016.
- [24] Sun S. R., Wang H. X., Mei D. H., Tu X., and Bogaerts A., CO<sub>2</sub> conversion in a gliding arc plasma: Performance improvement based on chemical reaction modeling, *J. CO<sub>2</sub> Util.*, Vol. 17, pp. 220–234, 2017.
- [25] Zlochower I. A., and Green G. M., The limiting oxygen concentration and flammability limits of gases and gas mixtures, *J. Loss Prev. Process Ind.*, Vol. 22 (4), pp. 499–505, 2009.
- [26] Center for Low Carbon Society Strategy, Survey on the carbon capture and storage process: Comparison of the chemical absorption process with the physical absorption process for CO<sub>2</sub> capture, *Proposal Paper for Policy Making and Governmental Action toward Low Carbon Society*, 2015.
- [27] Haruo K., Miyake K., and Sasano H., Development of PSA gas separation technology to reduce greenhouse effect, *Sumitomo Kagaku*, 2005.